610. Basic sets and attractors of a double swing power system

Y. Ueda[1,a], H. Ohta[2,b]
[1]Faculty of Science and Technology, Waseda University
Honorary Professor of the University of Aberdeen and Harbin Institute of Technology
Professor Emeritus of Kyoto University
Tokyo 169-0072, Japan
[2]Yatsukuchi-cho, Hanazono, Ukyo-ku, Kyoto 616-8053, Japan
e-mail: *[a]yueda@kurenai.waseda.jp, [b]hirofumi-ohta@masashi.ne.jp*

(Received 25 November 2010; accepted 4 February 2011)

Abstract. In a normal power system, many generators are operating in synchrony. That is, they all have the same speed or frequency, a system frequency. In the case of an accident a situation might occur when one or more generators are running at a different speed, at much faster than the system frequency. They are said to be stepping out. We have been engaged in a series of studies of this situation, and have found global attractor-basin portraits. The electric power system involving one generator operating into an infinite bus is a well-established model with a long history of research. We, however, have derived a new mathematical model, in which there is no infinite bus, nor fixed system frequency. In the simple case of two subsystems (each a swing pair) weakly coupled by an interconnecting transmission line, we have developed a system of seven differential equations, which include the variation of frequency in a fundamental way. We then go on to study the behavior of this model, using the straddle orbit method of computer simulation to find the basic set. We succeed in finding many basic sets in this new model. In addition, we consider unstable limit sets which have two- or three-dimensional outset.

Keywords: Power system stability; no infinite bus; basins of attraction; straddle orbit.

1. Introduction

We have been engaged in a series of studies of stepping out in electric power systems, and have not assumed an infinite bus having the nominal system frequency [Ueda et al., 2004]. That is, we do not fix the frequency of operation of the system, but instead take it as a dependent variable. This is determined by balancing the power generated with the power consumed in the electric power system. Our new mathematical model has not been found in other research works on electric power systems. In this paper we report on the basic sets of a model for a simple electric power system, consisting of two swing systems connected by a somewhat lower capacity interconnecting transmission line. By a swing system we mean a generator and motor pair, connected by a transmission line. Oscillation of the relative phases of the generator and the motor is similar to the simple pendulum of basic physics, so the two-swing system is similar to the double pendulum, or rather, two pendulums coupled by a spring.

In our most general model for the double swing system, we allow for arbitrary connection points for the transmission lines. We have introduced parameters to describe these connection points, and have established a model for this general case, as a system of seven differential equations [Ueda et al., 2004].

Then we specialize to two cases which we study in some detail (referred to as Case 1 and Case 2). As we will see below, Case 1 is a fairly idealized system and results in a subsystem of three dimensions that is independent of the rest of the system, which we call the frequency subsystem. In simulations we have determined that this subsystem has two attractors,

corresponding to synchronous and asynchronous operation between two power systems, respectively. We have found attractors in which one or the other or both of the swing systems are in static equilibrium or swing with smaller or larger amplitudes or step out. Then, using the straddle orbit method [Battelino et al., 1988], we carry out a series of simulation runs to organize our study. We find many basic sets (unstable equilibria or unstable limit cycles), and clarify connections among steady states. Next, based on the results of the Case 1 system as above, we carry out many simulation experiments for our more realistic Case 2 system.

Significant state from the viewpoint of normal operation in electric power system is only one stable equilibrium, and swinging (a stable limit cycle) or stepping out, which is caused by accidents, is abnormal and must not occur. In particular, basic sets (unstable equilibria or unstable limit cycles) have not been considered because they are not observed in real systems. For the purpose of stable operation, generators in the system are controlled so that swinging does not begin, or load or transmission line where an accident occurs is broken before leading to stepping out. In order to detect indication of swinging or stepping out, it is essentially important to take into consideration the fact that boundary between two states, including normal operation and swinging or stepping out, consists of a basic set, its insets, and its outset.

The paper is organized as follows. In Sec. 2 we summarize the derivation of the equations of motion of our new models. In Sec. 3 we discuss our Case 1 model, and describe its attractors and unstable limit sets. We also describe our preliminary simulations for basic sets. In Sec. 4, we use our knowledge of Case 1 to describe some of the basic sets for Case 2 systems. Finally, in Sec. 5, we summarize and present our conclusions.

2. Construction of the Electric Power System Model

In this section we summarize our new system, and compare with earlier works [Ueda et al., 2004].

2.1 The Interconnection of Two Systems

In Figure 1, we represent two generator/motor systems, labeled with subscripts 1 and 2, and tied by interconnecting transmission line, having inductance L. We assume ideal conditions, in that the generators and the motors are identical, the efficiency is 100%, and there is no loss in the step-up and step-down transformers nor in the transmission lines. The symbols indicated in Figure 1 are as follows. The points of connection of the interconnection line are determined by the parameters ℓ_1 and ℓ_2 ($0 \le \ell_1 \le 1$; $0 \le \ell_2 \le 1$) discussed below.

The rotating speeds (angular frequencies) of the two pairs are ω_1 and ω_2. The states of the four rotors are given by θ_{g1}, θ_{m1}, θ_{g2}, and θ_{m2}. The relative phases of the four rotors are given by γ_{g1}, γ_{m1}, γ_{g2}, and γ_{m2}. According to the familiar relations,

$$\begin{aligned} \theta_{g1} &= \omega_1 t + \gamma_{g1}, \;\; \theta_{m1} = \omega_1 t + \gamma_{m1} \\ \theta_{g2} &= \omega_2 t + \gamma_{g2}, \;\; \theta_{m2} = \omega_2 t + \gamma_{m2}. \end{aligned} \tag{1}$$

Note that here ω_1 and ω_2 are variables, rather than constants usually assumed, which are the angular velocities of the (commercial) infinite bus. In this research, we consider changes in both the angular frequencies and the relative phases, and we introduce assumptions that time variations of the relative phases may be neglected in comparison to the angular frequencies. We denote phase differences by,

$$\gamma_1 = \gamma_{g1} - \gamma_{m1}, \;\; \gamma_2 = \gamma_{g2} - \gamma_{m2}. \tag{2}$$

Mechanical power variables are P_{g1}, P_{m1}, P_{g2}, and P_{m2}, while the electric power variables are P_{ge1}, P_{me1}, P_{ge2}, and P_{me2}. In addition, we have flows of interchange power through the interconnection line from system 1 to system 2, P_{T1} and P_{T2}, as

$$P_{T1} = P_{ge1} - P_{me1}, \ P_{T2} = P_{me2} - P_{ge2}. \tag{3}$$

We assume that the angular frequency in each system does not change when the power imbalance is zero, we have,

$$\begin{aligned} 2I\frac{d\omega_1}{dt} &= \frac{1}{\omega_1}(P_{g1} - P_{m1} - P_{T1}) \\ 2I\frac{d\omega_2}{dt} &= \frac{1}{\omega_2}(P_{g2} - P_{m2} + P_{T2}) \end{aligned} \tag{4}$$

where I is the inertial moment equally of the generators, and of the motors.

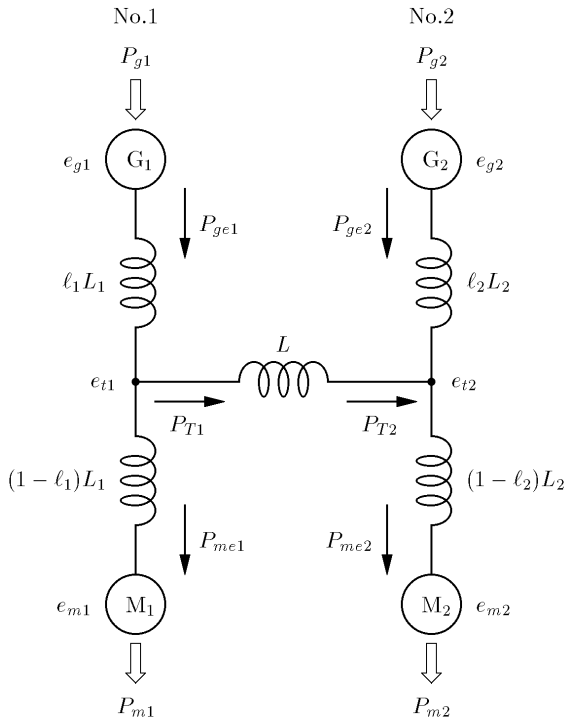

Fig. 1. Two swing systems are connected by an interchange transmission line of inductance, L. The parameters ℓ_1 and ℓ_2 determine the points at which the ends of the interchange line connect to the two swing pairs

Note that in this study, we consider systems consisting of generator/motor pairs, in which the generator and the motor have exactly the same capacity (our model might apply, for example, to a pumped-storage power station in which a large synchronous motor is used), and we assume that the coefficients of inertia of all four machines are identical.

2.2 Representation of Speed Governor and Load Characteristics

Because of the speed regulation characteristic of the governor, as the rotating speed decreases, the mechanical power input to the generator increases. Similarly, when the rotating speed increases, the mechanical power input to the generator decreases.

On the other hand, with an appropriate frequency characteristic of the load, as the frequency decreases, the power of the load decreases also, because the rotating speed of the motor decreases. And when the frequency increases, the power of the load increases. Such a frequency characteristic is called self-regulating. This is shown in Figure 2, where in addition, we have shown a characteristic which is approximately linear.

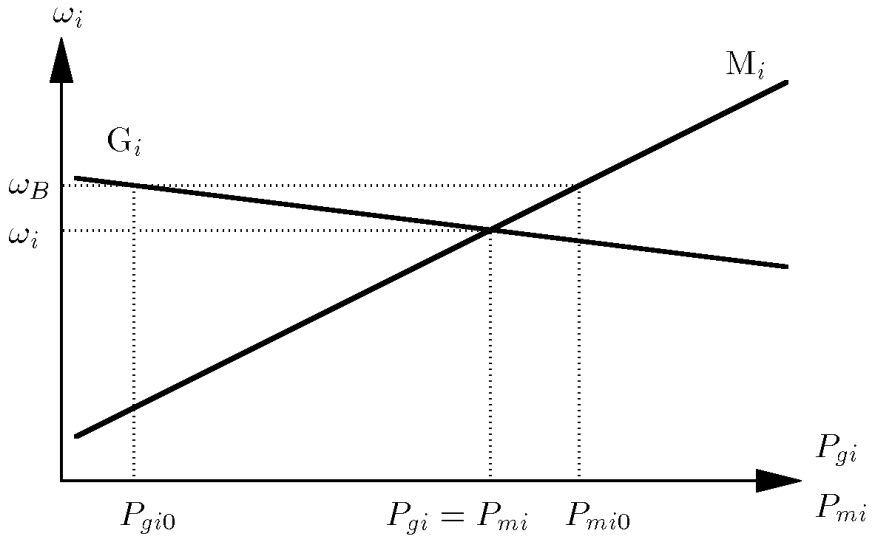

Fig. 2. Frequency characteristics of an electric power system. The speed regulation characteristic of the governor is labeled G. The self-regulation characteristic of the load is labeled M. Characteristic lines shown in the figure are applicable for neighborhood of actual equilibrium state

Mechanical power into the generator and that output by the motor depend thus on the frequencies of operation and the speed versus power characteristics of the generator and the motor, for which we assume the equations,

$$\begin{aligned} P_{gi} &= P_{gi0} + \%K_{gi} P_B(\omega_B - \omega_i)/2\pi \\ P_{mi} &= P_{mi0} + \%K_{mi} P_B(\omega_i - \omega_B)/2\pi \\ \omega_B &= 120\pi \end{aligned} \tag{5}$$

in which i = 1, 2 and the parameters appearing are: $\%K_{gi}$, speed/power characteristic of the generator, $\%K_{mi}$, speed/power characteristic of the motor, P_{gi0}, the set value of the mechanical power into the generator, P_{mi0}, the set value of the mechanical power output from the motor, P_B, the base power capacity of the system, and ω_B, the base angular frequency of the system. Here, we assume a 60 Hz system, see the last equation of (5).

2.3 Thévenin Equivalent Circuit

Figure 3 shows the Thévenin equivalent circuit of the two-swing system shown in Figure 1. Letting γ_{f1}, γ_{f2}, denote the phase differences of the fictitious voltages, e_{f1} and e_{f2}, against e_{m1} and e_{m2}, respectively, the fictitious voltages, e_{f1} and e_{f2}, are represented by the equations,

$$e_{fi} = \sqrt{2}E_{fi}\sin(\theta_{mi} + \gamma_{fi}) = (1-\ell_i)e_{gi} + \ell_i e_{mi}, \ (i = 1, 2) \tag{6}$$

where

$$\begin{aligned} E_{fi} &= E_i f_i \\ f_i &= \sqrt{\ell_i^2 + (1-\ell_i)^2 + 2\ell_i(1-\ell_i)cos\gamma_i} \\ \cos\gamma_{fi} &= \frac{\ell_i + (1-\ell_i)\cos\gamma_i}{f_i}, \ \sin\gamma_{fi} = \frac{(1-\ell_i)\sin\gamma_i}{f_i}, \ (i = 1, 2). \end{aligned} \tag{7}$$

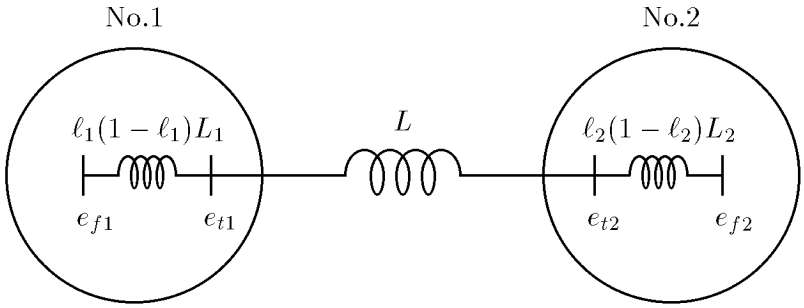

Fig. 3. Schematic diagram of the interconnection line in the two-swing system presented in Figure 1, showing equivalent circuits for the fictitious endpoints

We allow the angular speeds of the machines to depart slightly from the constant ω_B, so the amplitudes of the electromotive forces, which are proportional to the angular speeds, will be slightly different. That is, the following substitutions were used,

$$E_i = \frac{\omega_i}{\omega_B}E, \ (i = 1, 2). \tag{8}$$

Note that the fictitious voltages e_{f1} and e_{f2} are different from the voltages e_{t1} and e_{t2} at the endpoints of the interchange transmission line shown in Figure 1. The voltage, e_{f1}, is the fictitious voltage behind the fictitious inductance, $\ell_1(1-\ell_1)L_1$. Let

$$L_{12} = L + \ell_1(1-\ell_1)L_1 + \ell_2(1-\ell_2)L_2. \tag{9}$$

Note also here that the absolute values of the fictitious voltages e_{f1} and e_{f2} may vary, as they depend on the power input to and output from the system, and on the positions of the endpoints of the interconnecting transmission line, that is, on the parameters ℓ_1 and ℓ_2.

Finally, let γ_{12} denote the phase difference of e_{f1} against e_{f2} as

$$\gamma_{12} = \theta_{m1} + \gamma_{f1} - (\theta_{m2} + \gamma_{f2}). \tag{10}$$

Then appealing to the assumptions for the relative phases, we have from (1),

$$\frac{d\gamma_{12}}{dt} = \omega_1 - \omega_2. \tag{11}$$

2.4 Differential Equations Describing the System

Applying circuit theory analysis, we may calculate the electric power flows P_{ge1}, P_{me1}, P_{ge2}, and P_{me2} in the circuit. Then with swing equations, we have the differential equations describing the system indicated in Figure 1,

$$\begin{aligned}
\frac{d\gamma_1}{d\tau} &= \chi_1 \\
\frac{d\chi_1}{d\tau} &= \frac{\omega_B}{\omega_1}\{p_{g10} + p_{m10} + k_1^-(\omega_B - \omega_1)\} - 2b_{12}\ell_1 f_2 \sin(\gamma_{f1} - \gamma_{12}) \\
&\quad -b_{12} f_1 f_2 \sin\gamma_{12} + 2b_{12}\ell_1 f_1 \sin\gamma_{f1} - 2b_1 \sin\gamma_1 - D_1\chi_1 \\
\frac{d\gamma_2}{d\tau} &= \chi_2 \\
\frac{d\chi_2}{d\tau} &= \frac{\omega_B}{\omega_2}\{p_{g20} + p_{m20} + k_2^-(\omega_B - \omega_2)\} - 2b_{12}\ell_2 f_1 \sin(\gamma_{f2} + \gamma_{12}) \\
&\quad +b_{12} f_1 f_2 \sin\gamma_{12} + 2b_{12}\ell_2 f_2 \sin\gamma_{f2} - 2b_2 \sin\gamma_2 - D_2\chi_2 \\
\frac{d\gamma_{12}}{d\tau} &= \frac{1}{a}(\omega_1 - \omega_2) \\
\frac{d\omega_1}{d\tau} &= \frac{a}{2}\left[\frac{\omega_B}{\omega_1}\{p_{g10} - p_{m10} + k_1^+(\omega_B - \omega_1)\} - b_{12} f_1 f_2 \sin\gamma_{12}\right] \\
\frac{d\omega_2}{d\tau} &= \frac{a}{2}\left[\frac{\omega_B}{\omega_2}\{p_{g20} - p_{m20} + k_2^+(\omega_B - \omega_2)\} + b_{12} f_1 f_2 \sin\gamma_{12}\right]
\end{aligned} \tag{12}$$

with

$$\tau = at, \ a = \sqrt{\frac{P_B}{\omega_B I}} \tag{13}$$

and

$$\begin{aligned}
b_i = \frac{E^2}{\omega_B L_i P_B}, \ b_{12} = \frac{E^2}{\omega_B L_{12} P_B}, \ D_i = c_i\sqrt{\frac{\omega_B}{P_B I}} \\
k_i^- = \frac{\%K_{gi} - \%K_{mi}}{2\pi}, \ k_i^+ = \frac{\%K_{gi} + \%K_{mi}}{2\pi} \\
p_{gi0} = \frac{P_{gi0}}{P_B}, \ p_{mi0} = \frac{P_{mi0}}{P_B} \ (i = 1, 2).
\end{aligned} \tag{14}$$

Note. In the situation in which the two generator/motor pair systems lose synchrony, the interchange powers, P_{T1} and P_{T2}, begin to swing. But in this derivation we have included only the lowest frequency term of their power swing components.

3. Simulation of the System for Case 1

In this section we provide some considerations regarding the system of equations obtained in the preceding section. We consider the special case called Case 1 in the first section.

3.1 Differential Equations

We now consider Case 1, shown in Figure 4, in which $\ell_1 = 1$, $\ell_2 = 0$. Our equations (11) now reduce to,

$$\begin{aligned}
\frac{d\gamma_1}{d\tau} &= \chi_1 \\
\frac{d\chi_1}{d\tau} &= \frac{\omega_B}{\omega_1}\left\{p_{g10} + p_{m10} + k_1^-(\omega_B - \omega_1)\right\} + b_{12}\sin\gamma_{12} - 2b_1\sin\gamma_1 - D_1\chi_1 \\
\frac{d\gamma_2}{d\tau} &= \chi_2 \\
\frac{d\chi_2}{d\tau} &= \frac{\omega_B}{\omega_2}\left\{p_{g20} + p_{m20} + k_2^-(\omega_B - \omega_2)\right\} + b_{12}\sin\gamma_{12} - 2b_2\sin\gamma_2 - D_2\chi_2 \\
\frac{d\gamma_{12}}{d\tau} &= \frac{1}{a}(\omega_1 - \omega_2) \\
\frac{d\omega_1}{d\tau} &= \frac{a}{2}\left[\frac{\omega_B}{\omega_1}\left\{p_{g10} - p_{m10} + k_1^+(\omega_B - \omega_1)\right\} - b_{12}\sin\gamma_{12}\right] \\
\frac{d\omega_2}{d\tau} &= \frac{a}{2}\left[\frac{\omega_B}{\omega_2}\left\{p_{g20} - p_{m20} + k_2^+(\omega_B - \omega_2)\right\} + b_{12}\sin\gamma_{12}\right].
\end{aligned} \tag{15}$$

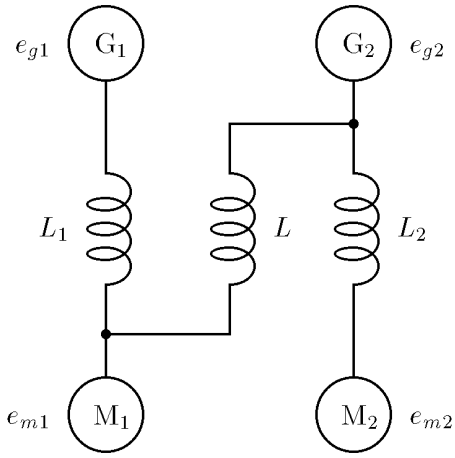

Fig. 4. Schematic diagram for the two-swing system in our special Case 1

Note. Taking $\ell_1 = 1$ corresponds to placing the bus inside the motor of the first generator/motor pair, where the electromotive force is e_{m1}. But this is impossible in practice. Similar considerations apply to $\ell_2 = 0$. In this study, control devices such as AVR, PSS, and governor dynamics, are excluded.

3.2 Establishment of Parameters

The values of system parameter that we use in the simulation experiments of this section are,

$$\begin{aligned} a = 6.0, \quad & D_1 = D_2 = 0.005 \\ b_{12} = 0.1, \quad & b_1 = b_2 = 1.25 \\ k_1^- = k_2^- = \frac{3}{200\pi}(= k^-), \quad & k_1^+ = k_2^+ = \frac{1}{40\pi}(= k^+) \end{aligned} \tag{16}$$

where some parameters are made equal: $c_1 = c_2$, $k_{g1} = k_{g2}$ ($= k_g$), $k_{m1} = k_{m2}$ ($= k_m$), and $L_1 = L_2$. We now set values for the mechanical power input to, and the mechanical power output from, each of the two swing systems:

$$\begin{aligned} p_{g10} = 0.45, \quad & p_{m10} = 0.40 \\ p_{g20} = 0.40, \quad & p_{m20} = 0.45. \end{aligned} \tag{17}$$

Then, values for the power imbalance are,

$$p_{10} = p_{g10} - p_{m10} = 0.05, \; p_{20} = p_{g20} - p_{m20} = -0.05 \tag{18}$$

We assume that the transmission power capacity of the interconnection line is fairly small than the steady state stability limit of either of the two swing systems. We establish the speed regulation of the governor, and the self-regulation of the load. We chose values for parameters – for example, k_g and k_m, and the slopes in Figure 2 – to facilitate the observation of frequency deviations, rather than for fidelity to realistic systems. The equivalent circuits chosen for the generators and motors are relatively simple. Other parameters have been selected more realistically.

3.3 Steady States of the System

We now understand the dynamics of the system in Case 1 as follows.

The first two equations of (15) represent the first swing system, and the third and fourth equations represent the second swing system. The lower three equations of the frequency subsystem are separated, in the sense that in these three lower equations, the variables of the upper four equations do not appear. On the other hand, the variables of the lower frequency subsystem do appear in the upper four equations. The systems 1 and 2 are also separated from each other, in the sense that in the equations of one system, the variables of the other system do not appear.

Thus, when the lower subsystem settles into a point attractor (static equilibrium), its variables settle to constant values, and appear in the two upper subsystems as constant forcing (bias) terms. On the other hand, when the lower subsystem settles into a periodic attractor (that

is, a limit cycle, or oscillation), its variables appear in the two upper subsystems as periodic forcing terms. The other can also settle into a static equilibrium when one system steps out.

In the following, we describe the steady states found in the system, Case 1. We use the term steady states to include both stable and unstable limit sets. Attractors are classified in Table 1, basic sets (unstable steady states which have a one-dimensional outset) are classified in Table 2, and unstable steady states which have a two- or three-dimensional outset are classified in Table 3. The attractors described here are obtained by simulation from the mathematical model specified by Eqs. (15), and may not be always observed in actual electric power systems.

3.3.1 Steady States with Synchrony of the Two Swing Systems

In the case in which the two swing systems are in synchrony, that is, $\omega_1 = \omega_2 = 120\pi$, each of the swing systems behaves independently as follows. γ_{12} is also constant, that is, $\gamma_{12} = \pi/6$ is stable, and $\gamma_{12} = 5\pi/6$ is unstable.

Table 1. Attractors in the System for Case 1

No.	Abbr.	System 1	System 2	Between Systems
1	EE	Equilibrium	Equilibrium	Synchrony (Equilibrium)
2	EO	Equilibrium	Stepping-Out	
3	OE	Stepping-Out	Equilibrium	
4	OOs	Stepping-Out	Stepping-Out	
5	SS	Small Amplitude	Small Amplitude	Asynchrony
6	SL	Small Amplitude	Large Amplitude	
7	LS	Large Amplitude	Small Amplitude	
8	LL	Large Amplitude	Large Amplitude	
9	SO	Small Amplitude	Stepping-Out	
10	OS	Stepping-Out	Small Amplitude	
11	LO	Large Amplitude	Stepping-Out	
12	OL	Stepping-Out	Large Amplitude	
13	OOa	Stepping-Out	Stepping-Out	

Table 2. Basic sets in the System for Case 1

No.	Abbr.	System 1	System 2	Between Systems
14	UE	Unstable Equilibrium	Equilibrium	Equilibrium
15	EU	Equilibrium	Unstable Equilibrium	Equilibrium
16	EEu	Equilibrium	Equilibrium	Unstable Equilibrium
17	UOs	Unstable Equilibrium	Stepping-Out	Equilibrium
18	EOu	Equilibrium	Stepping-Out	Unstable Equilibrium
19	OUs	Stepping-Out	Unstable Equilibrium	Equilibrium
20	OEu	Stepping-Out	Equilibrium	Unstable Equilibrium
21	OOu	Stepping-Out	Stepping-Out	Unstable Equilibrium
22	SU	Small Amplitude	Unstable Large	Asynchrony
23	US	Unstable Large	Small Amplitude	
24	UL	Unstable Large	Large Amplitude	
25	LU	Large Amplitude	Unstable Large	
26	UOa	Unstable Large	Stepping-Out	
27	OUa	Stepping-Out	Unstable Large	

Table 3. Unstable steady states which have two- or three-dimensional outset in the System for Case 1

No.	Abbr.	System 1	System 2	Between Systems
28	UEu	Unstable Equilibrium	Equilibrium	Unstable Equilibrium
29	EUu	Equilibrium	Unstable Equilibrium	Unstable Equilibrium
30	UUs	Unstable Equilibrium	Unstable Equilibrium	Equilibrium
31	UUu	Unstable Equilibrium	Unstable Equilibrium	Unstable Equilibrium
32	UOu	Unstable Equilibrium	Stepping-Out	Unstable Equilibrium
33	OUu	Stepping-Out	Unstable Equilibrium	Unstable Equilibrium
34	UUa	Unstable Large	Unstable Large	Asynchrony

System 1 is in a stable equilibrium ($\gamma_1 \simeq 0.368268$; $\chi_1 = 0$), or steps out (γ_1 increases indefinitely, but a limit cycle on cylindrical state space). System 2 is also either in a stable equilibrium ($\gamma_2 \simeq 0.368268$; $\chi_2 = 0$), or steps out (γ_2 increases indefinitely, but a limit cycle on cylindrical state space). Thus, for the whole system, this case comprises four attractors: No. 1 to 4 in Table 1. Each system also has an unstable equilibrium ($\gamma_1, \gamma_2 \simeq 2.773325$). With $\gamma_{12} = 5\pi/6$, there are seven unstable equilibria (both systems are in the equilibria): No. 14 to 16 in Table 2 and No. 28 to 31 in Table 3, and seven unstable steady states (one or two systems step out): No. 17 to 21 in Table 2 and No. 32 and 33 in Table 3.

3.3.2 Steady States with Asynchrony of the Two Swing Systems

In this case, the phases of the two systems are not locked, and γ_{12} increases without bound. The term $b_{12}\sin\gamma_{12}$ acts as a periodic forcing term in each of the two swing subsystems. Each then occupies one of the three states: swinging with small amplitude, swinging with large amplitude, or stepping out (γ_1 or γ_2 increases indefinitely). Thus, for the whole system, this case comprises nine attractors: No. 5 to 13 in Table 1, and seven unstable steady states: No. 22 to 27 in Table 2 and No. 34 in Table 3.

A time series of γ_1, γ_2, and γ_{12} for the LL, LU, and UL are shown in Figure 5, and those for

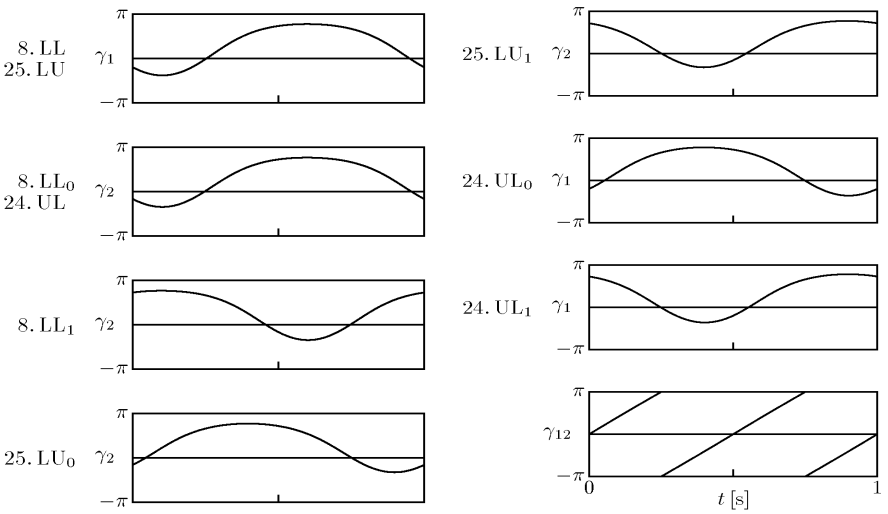

Fig. 5. Time series for the attractor LL and the basic set LU and UL. γ_1's of the LL_0, LL_1, LU_0, and LU_1 are identical, γ_2's of the LL_0, UL_0, and UL_1 are identical, and γ_{12}'s of the all are identical. The waveform of swinging with unstable large amplitude (U) is slightly different from that of swinging with stable large amplitude (L), and the waveform of the system 2 is slightly different from that of the system 1

the SL, SU, LS, and US are shown in Figure 6(a). We explain Figure 6(b) in the next section. The period of γ_1 and γ_2 for small amplitude ($\simeq$ 0.5 [s]) is the same as that of γ_{12}, and that for large amplitude ($\simeq$ 1[s]) is double. Therefore, recalling that two systems are separated from each other, if both systems swing with large amplitude, it is possible to shift the phase of one system (γ_2 against γ_1) by half period; the LL, UL, LU, and UUa are further classified into two steady states respectively. The phase difference between two systems is 0 or half period ($\simeq$ 0.5 [s]) for the LL, and for the UL and LU, about –0.2 [s] or about 0.3 [s]. The SU and US are also different from the SL and LS respectively not only in stability but also in phase.

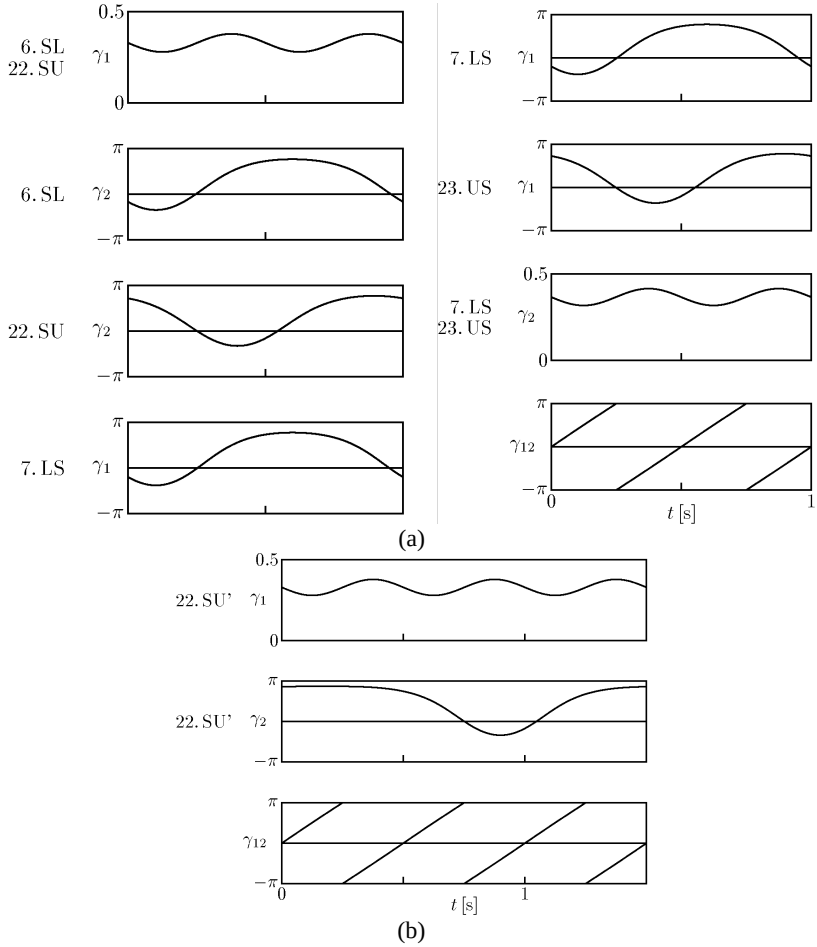

Fig. 6. Time series for the attractor SL and LS and the basic set SU, US, and SU'. γ_1's of the SL and SU are identical, γ_2's of the LS and US are identical, and γ_{12}'s of the all are identical. The slight differences among waveforms are similar to Figure 5

3.4 Connections among Steady States

We now investigate basic sets by using the straddle orbit method. The results are illustrated in Figure 7. The definitions of panels in the figure are shown in Figure 7(e), and the steady states, No. 28, 29, 32, and 33, are not basic sets, and we explain them in Sec. 3.6. The results are summarized in the following laws:

(1) In a system, the basic set between the equilibrium and the stepping out in synchrony is the unstable equilibrium with respect to the system (γ_1 or $\gamma_2 \simeq 2.773325$). This case comprises four steady states: the UE, EU, UOs, and OUs.

(2) The basic set between synchrony and asynchrony is related to the unstable equilibrium between systems ($\gamma_{12} = 5\pi/6$); the equilibrium and the small amplitude limit cycle are interchanged. This case comprises four steady states: the EEu, EOu, OEu, and OOu.

(3) In a system, the basic set between the small amplitude and the stepping out in asynchrony may be composed of two unstable large amplitude limit cycles with respect to the system. We explain them in this section later. This case comprises six steady states: No. 22 to 27 in Table 2.

Although 91 combinations of two attractors are possible because there are 14 attractors (Table 1 and two cases of the LL), only 14 combinations bring basic sets (Table 2 and Figure 7). For the other combinations, the middle point between a pair of points on the straddle orbit converges to another attractor. For example, the middle point between the EE and SO converges to the EO, and this is understood from Figure 7. For another example, the middle point between the EE and OOs converges to the EO or OE, and we further consider this in Sec. 3.6. The limit cycles of Figures 7(a), (b), and (c) are separated from one another. Limit cycles including large amplitude do not appear in Figure 7(a), and two cases of the LL, which are shown in Figure 7(d), do not appear in Figures 7(a), (b), and (c). These are due to that all the middle points between any large amplitude attractor and the other attractor converge to another attractor.

The six basic sets with asynchrony, which are in case (3), are shown by three pairs of two panels in Figure 7; two unstable limit cycles are shown on the top and the bottom, and a typical example of the straddle orbit is presented on the middle. These unstable limit cycles have only one characteristic multiplier whose absolute value is greater than 1; its outset is one-dimensional. Note that the UL and LU have two cases respectively as indicated in Figure 5. The straddle orbit appears to be chaotic, and finally the middle point between a pair of points on the straddle orbit converges to another attractor (the "chaotic" straddle orbits are drawn in the figure with the point that is half as large as the others). We denote such phenomena by dotted lines in the figures, and consider them in the next section. That is, only in the case of No. 14 to 21 in Table 2, to which two solid lines are attached in Figure 7(a), the point on the straddle orbit did converge to the basic set.

In the case of four straddle orbits, which are in case (3), shown in Figure 7(a), the point on the straddle orbit repeats to stay on the SU, US, UOa, or OUa for ten or more cycles, to depart from it, to approach the SU', U'S, U'Oa, or OU'a, and to return to the former after the point moves along the latter for one cycle (rarely two cycles). This is explained by the fact that, for example, the largest characteristic multiplier of the SU' is about 176, on the other hand, the SU 3.4. Figure 6(b) shows a time series of γ_1, γ_2, and γ_{12} for the SU'. The unstable limit cycle U' is three times longer than the period of γ_{12}, and the unstable limit cycle U is twice than the period of γ_{12}. The "chaotic" straddle orbit may involve other unstable limit cycles, and the period of limit cycles needs to be an integer multiple of the period of γ_{12}. As long as we examine, it does not seem that other unstable limit cycles exist.

In the case of the straddle orbit shown in Figure 7(b) or 7(c), the point on the straddle orbit wanders between UL_0 and UL_1 or between LU_0 and LU_1, and stays on them for ten or more cycles. Although the point seems to approach the U'L or LU' while it transfers to the other, it does not stay on the U'L or LU' for even one cycle; neither U'L nor LU' is impossible because the limit cycle L is twice longer than the period of γ_{12}, on the other hand, the U' is three times longer.

In the case of the straddle orbit between the SL and SO, for example, the middle point between a pair of points on the straddle orbit converges to the SS early. When the middle point has converged to the SS, by replacing the middle point with another ratio of dividing between a

pair of points on the straddle orbit, we can get the straddle orbit for a long time relatively. The straddle orbit seems to approach the SU before it converges to the SS, it however stays on no closed curves for even one cycle. This is similar to the other straddle orbits between the large amplitude L and the stepping out O, and this is not observed at the other combinations, such as the small amplitude S and the large amplitude L; straddle orbits converge to another attractor early even if replacing it.

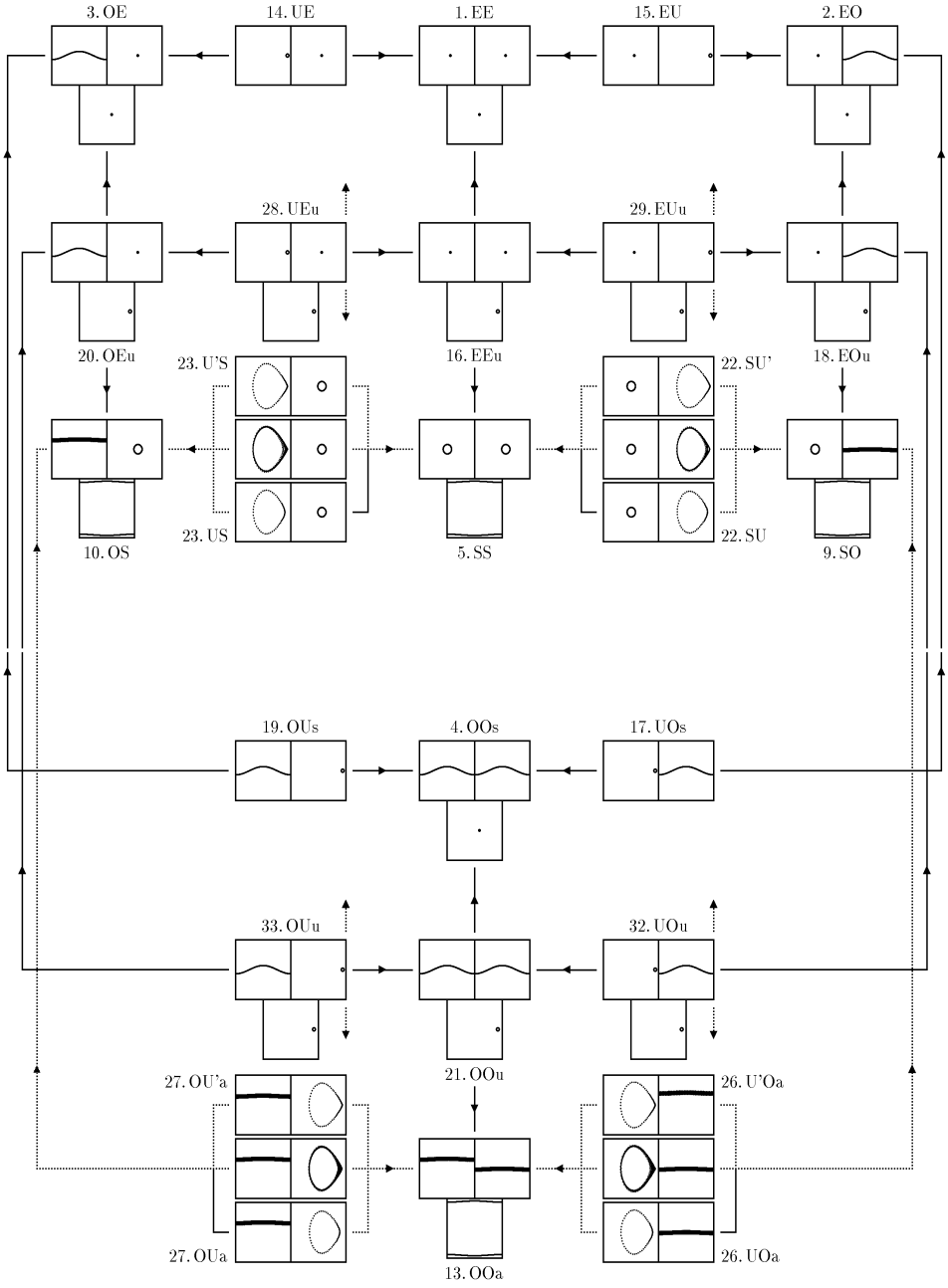

(a)

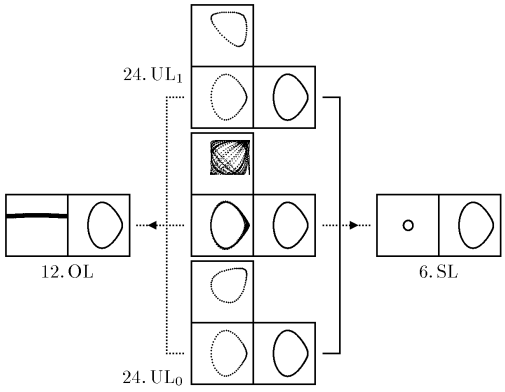

(b)

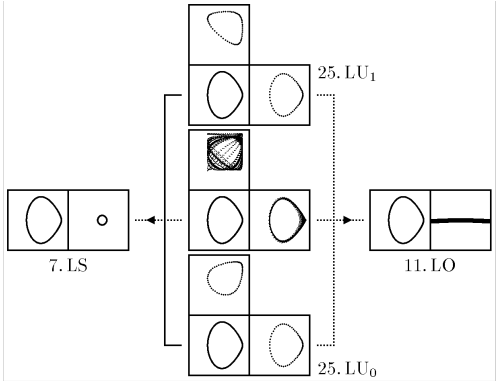

(c)

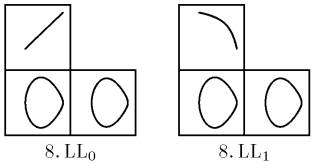

(d)

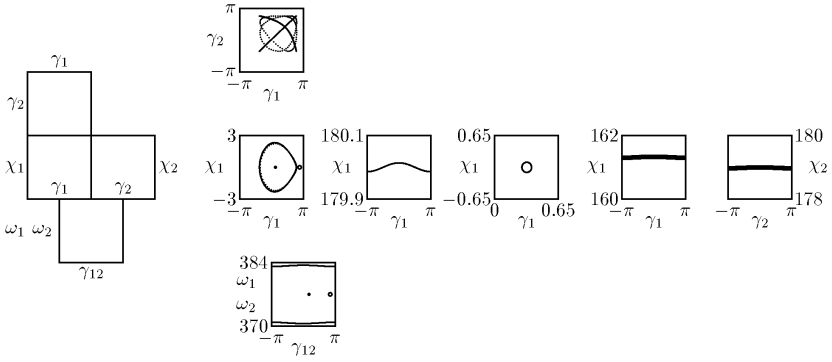

(e)

Fig. 7. Connection among steady states for Case 1

3.5 Fractal Basin Boundary

In the case (3), although outset of each unstable limit cycle is one-dimensional, a pair of points on a straddle orbit departs from the limit cycle, and the middle point converges to another attractor. For example, a pair of points on a straddle orbit between the SS and SO wanders between the SU and SU', and finally the middle point converges to the SL.

The outset of a point x_0 on the SU is one-dimensional (the characteristic multiplier is 3.3716), and its first approximation is given by the eigenvector v. Let x_0 be the point which corresponds to the time origin of the SU in Figure 6, the γ_2 component of v be positive, and $|v| = 1$. We determine whether the point

$$\boldsymbol{x_1 = x_0 + kv} \tag{19}$$

converges to the SS or SO depending on k, and the result is provided in Figure 8(a). In the figure, the abscissa represents k, and the ordinate represents the No. of attractors shown in Table 1. For $k < 0$, all the points always converge to the SS, and this is the reason why the line which begins at the left of the SU is solid; this rule is applicable to the others. For $k > 0$, although the points almost converge to the SO, some of them converge to the SS, and one or two converge to the SL. It has been confirmed by enlarging the figure that the basin boundary is fractal. We also show the similar for the SU' in Figure 8(b). Note that the point at – 0.0005 converges to the SL in the top of the figure and that the point at –0.000003 converges to the SL in the bottom although we do not point arrows at them in the figure. In these cases, the middle point between a pair of points on the straddle orbit finally converges to the SL. However it will be possible to prevent the point from converging by another ratio of dividing between a pair of points on the straddle orbit. The SU and SU' seem to be a heteroclinic connection, and this will be the reason why the straddle orbit wanders.

Note that, in the case of No. 14 to 21 in Table 2, the point always converges to an attractor for $k > 0$, and for $k < 0$, it always converges to another attractor, that is, the basin boundary is $k = 0$ only. Basins may also differ from the figures a little due to the method of numerical integration, the time step, or the choice of x_0.

3.6 Two- or Three-Dimensional Outsets

The unstable equilibria, UEu, EUu, and UUs, and the unstable steady states, UOu, OUu, and UUa, have a two-dimensional outset. The unstable steady state, UUu, has a three-dimensional outset.

One of the two one-dimensional outsets of the UEu has components for γ_1 and χ_1 only. γ_{12} can remain at $5\pi/6$, which is unstable, because it is separated from γ_1 and χ_1, and the right-hand sides of the lower three equations of (15) are exactly 0, and we can trace the outset. One direction of the outset connects to one of insets of the OEu, and the other direction connects to one of insets of the EEu. This is presented in Figure 7(a) with the cases of the EUu, UOu, and OUu. It is difficult to trace the other outset of the UEu, EUu, UOu, and OUu.

There is the case that a pair of points on a straddle orbit between the EE and OOs approaches the UUs before the middle point converges to the EO or OE. One of the eigenvalues of the equilibrium UUs is equal root, 1.5247, and the dimension of its eigenspace is two, that is, the outset is a two-dimensional invariant surface. This outset touches insets of the EE, OOs, EO, and OE. For the UUs, we examine x_1 described by Eq. (19). It converges to the EE or OOs for some eigenvectors, and for others, it converges to the EO or OE. Basin boundaries are also $k = 0$ only.

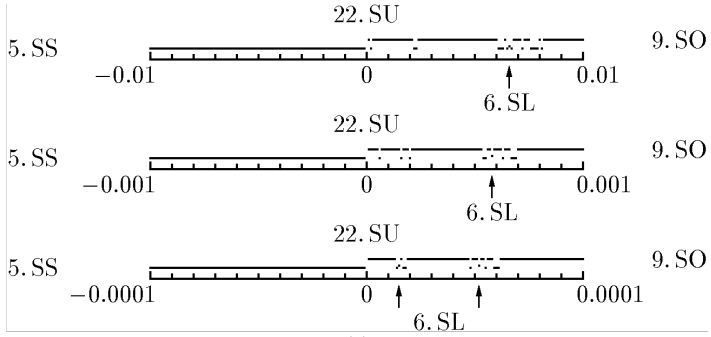

(a)

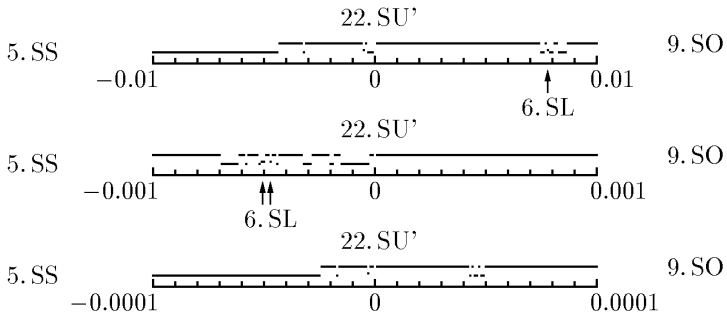

(b)

Fig. 8. Attractor-basin of SS or SO with 200 grids of the lengths of eigenvector on the basic set SU or SU'; the abscissa represents the length and the ordinate represents the No. of attractors

Since the UUa (in asynchrony) corresponds to the UUs (in synchrony), it seems that the outset of the UUa touches insets of the SS, OOa, SO, and OS. However, we were unable to find the case in which a pair of points on a straddle orbit approaches the UUa, and x_1 did not converge to the SS although it converges to the OOa (and SO, OS, LO, and OL). No characteristic multiplier of the UUa is also equal root (3.3003 for system 1 and 3.3716 for system 2).

The outset of the UUu is composed of a two-dimensional invariant surface and a one-dimensional invariant curve. The surface touches insets of the EEu, OOu, EOu, and OEu. Since it is difficult to trace the curve, we examine the corresponding x_1. One direction converges to the EE, and the other converges to the SO, OS or OOa.

4. Simulation of the System for Case 2

With the above results for Case 1 in mind, we now proceed to investigation of Case 2, as shown in Figure 1, by simulation.

4.1 Differential Equations

We consider the case in which, referring to Figure 1, the buses of the interconnecting transmission line are located at the midpoints of the two swing pairs. That is, we set, $\ell_1 = \ell_2 = 0.5$. This defines our Case 2. Then the differential equations (11) become the following,

$$\begin{aligned}
\frac{d\gamma_1}{d\tau} &= \chi_1 \\
\frac{d\chi_1}{d\tau} &= \frac{\omega_B}{\omega_1}\left\{p_{g10} + p_{m10} + k_1^-(\omega_B - \omega_1)\right\} - b_{12}\sin\frac{\gamma_1}{2}\cos\frac{\gamma_2}{2}\cos\gamma_{12} - 2b_{11}\sin\gamma_1 - D_1\chi_1 \\
\frac{d\gamma_2}{d\tau} &= \chi_2 \\
\frac{d\chi_2}{d\tau} &= \frac{\omega_B}{\omega_2}\left\{p_{g20} + p_{m20} + k_2^-(\omega_B - \omega_2)\right\} - b_{12}\cos\frac{\gamma_1}{2}\sin\frac{\gamma_2}{2}\cos\gamma_{12} - 2b_{22}\sin\gamma_2 - D_2\chi_2 \\
\frac{d\gamma_{12}}{d\tau} &= \frac{1}{a}(\omega_1 - \omega_2) \\
\frac{d\omega_1}{d\tau} &= \frac{a}{2}\left[\frac{\omega_B}{\omega_1}\left\{p_{g10} - p_{m10} + k_1^+(\omega_B - \omega_1)\right\} - b_{12}\cos\frac{\gamma_1}{2}\cos\frac{\gamma_2}{2}\sin\gamma_{12}\right] \\
\frac{d\omega_2}{d\tau} &= \frac{a}{2}\left[\frac{\omega_B}{\omega_2}\left\{p_{g20} - p_{m20} + k_2^+(\omega_B - \omega_2)\right\} + b_{12}\cos\frac{\gamma_1}{2}\cos\frac{\gamma_2}{2}\sin\gamma_{12}\right].
\end{aligned} \tag{20}$$

where,

$$b_{ii} = \frac{E^2}{\omega_B L_i P_B}\left(1 - \frac{L_i}{4L_{12}}\right) = b_i - \frac{b_{12}}{4}, (i = 1, 2). \tag{21}$$

Looking at Eqs. (20) for Case 2 in comparison with the corresponding equations for Case 1, we see two complicating factors.

First, the three-dimensional frequency subsystem is no longer separated. That is, variables of the two swing subsystems now appear in them. Secondly, the first swing system (represented by the first and second equations) and the second swing system (represented by the third and fourth equations) are no longer uncoupled. That is, variables of each appear in the other. In sum, we have in Case 2 a fully coupled system. Physically, this may be understood as a necessary consequence of the fact that the bus voltages are no longer constant, as in Case 1.

Note. Eqs. (20) hold for $-\pi \le \gamma_1 \le \pi$ and $-\pi \le \gamma_2 \le \pi$.

4.2 Setting up Parameters

For Case 2, we set the system parameters as follows,

$$\begin{aligned}
a &= 6.0, \quad D_1 = D_2 = 0.005 \\
b_{12} &= 0.1, \quad b_{11} = b_{22} = 1.225 \\
k_1^- = k_2^- &= \frac{3}{200\pi}, \quad k_1^+ = k_2^+ = \frac{1}{40\pi}
\end{aligned} \tag{22}$$

where as in Case 1, some parameters are made equal: $c_1 = c_2$, $k_{g1} = k_{g2}$, $k_{m1} = k_{m2}$, and $L_1 = L_2$.

Note that these are almost the same as the system parameters chosen for the simulation of Case 1. This allows us to make use of our results for Case 1 in predicting the behavior of Case2.

And we now set the power parameters as,

$$\begin{aligned}
p_{g10} &= 0.45, \quad p_{m10} = 0.40 \\
p_{g20} &= 0.40, \quad p_{m20} = 0.45.
\end{aligned} \tag{23}$$

4.3 Steady States of the System

As described in Sec. 3.3, we use the term steady states to include both stable and unstable limit sets, and they are classified in Table 1 to 3 for Case 1. Some of them do not exist in Case 2, and we examine this by decreasing ℓ_1 (= 1 for Case 1) and $\ell_2 = 1 - \ell_1$ as follows.

The pair of the EU and EUu and the pair of the UE and UEu disappear at $\ell_1 = 0.7382$ by saddle-node bifurcation, where the saddle-node implies that unstability-stability with respect to γ_{12}. This type of saddle-node bifurcation also leads the UUs and UUu to disappear at $\ell_1 = 0.8469$. Therefore, only the EE and EEu are equilibria.

This type of saddle-node bifurcation also leads the OOs and OOu to disappear at $\ell_1 = 0.5032$, the pair of the UOs and UOu and the pair of the OUs and OUu at $\ell_1 = 0.7984$.

The eight steady states which represent that both the systems are swinging with large amplitude do not exist. The LL_0 and LU_0 (see Figure 5) disappear at $\ell_1 = 0.5574$ by cyclic fold bifurcation, where the cyclic fold implies that the limit cycle with the large amplitude and the limit cycle with the unstable large amplitude in the system 2. This type of cyclic fold bifurcation also leads the LL_1 and UL_1 to disappear at $\ell_1 = 0.8140$, the UUa_1 and LU_1 at $\ell_1 = 0.7546$, and the UUa_0 and UL_0 at $\ell_1 = 0.6786$.

That is, No. 1 to 3, 5 to 7, 9 to 13, 16, 18, 20, 22, 23, 26, 27 exist in Table 1 to 3.

4.4 Connections among Steady States

We now investigate basic sets by using the straddle orbit method. The results are illustrated in Figure 9. The definitions of panels in the figure are shown in Figure 7(e) except stepping out and swinging with small amplitude, which are shown in Figure 9. The SL and LS are isolated from the other limit cycles. The small amplitude S with the large amplitude L, U, or U' is twofold; the part that looks thick consists of two little separated lines. These are due to that all the middle points between a pair of points on the straddle orbits between them and the other attractor converge to another attractor. We also note that the middle point between the EE and EO converges to the SO, and that the middle point between the EE and OE converges to the OS. In such cases, by regarding attractors as the EE, which represents normal operation of the power system, and the others, the straddle orbits converge to the EEu; the attractor basin boundary of the EE is considered as the EEu.

The basic sets between the SS and SO, and between the SS and OS are similar to Case 1. The point on the straddle orbit alternates staying on the SU (or US) and the SU' (or U'S) only one or two cycles, which are different from Case 1. The largest characteristic multiplier of the U'S is about 141, the SU' 124, on the other hand, the US 2.7, the SU 2.6.

The UOa and OUa are the basic sets between the SO and LO and between the OS and OL, respectively; the basic set between the small amplitude and the large amplitude is the unstable limit cycle U. On the other hand, the basic sets between the OOa and SO and between the OOa and OS are not the U'Oa and OU'a, but involve them respectively. These are confirmed by the enlarged views of the most right part, $[17\pi/20; 18\pi/20] \times [-0.15; 0.15]$, shown below the panel of the large amplitude of the straddle orbit. Note that the large amplitudes of the straddle orbits are about 70 cycles, and that the middle point between a pair of points on the straddle orbit finally converges to another attractor. Figure 10(a) shows a part of the straddle orbit and the enlarged views of the most right part, $[53\pi/60; 54\pi/60] \times [-0.05; 0.05]$, and Figure 10(b) shows its time series. Although the orbit seems to stay on a closed curve for three cycles and the curve is four times longer than the period of γ_{12}, we have not been able to identify the closed curve as an unstable limit cycle. The basic sets between the OOa and SO and between the OOa and OS will involve such limit cycles.

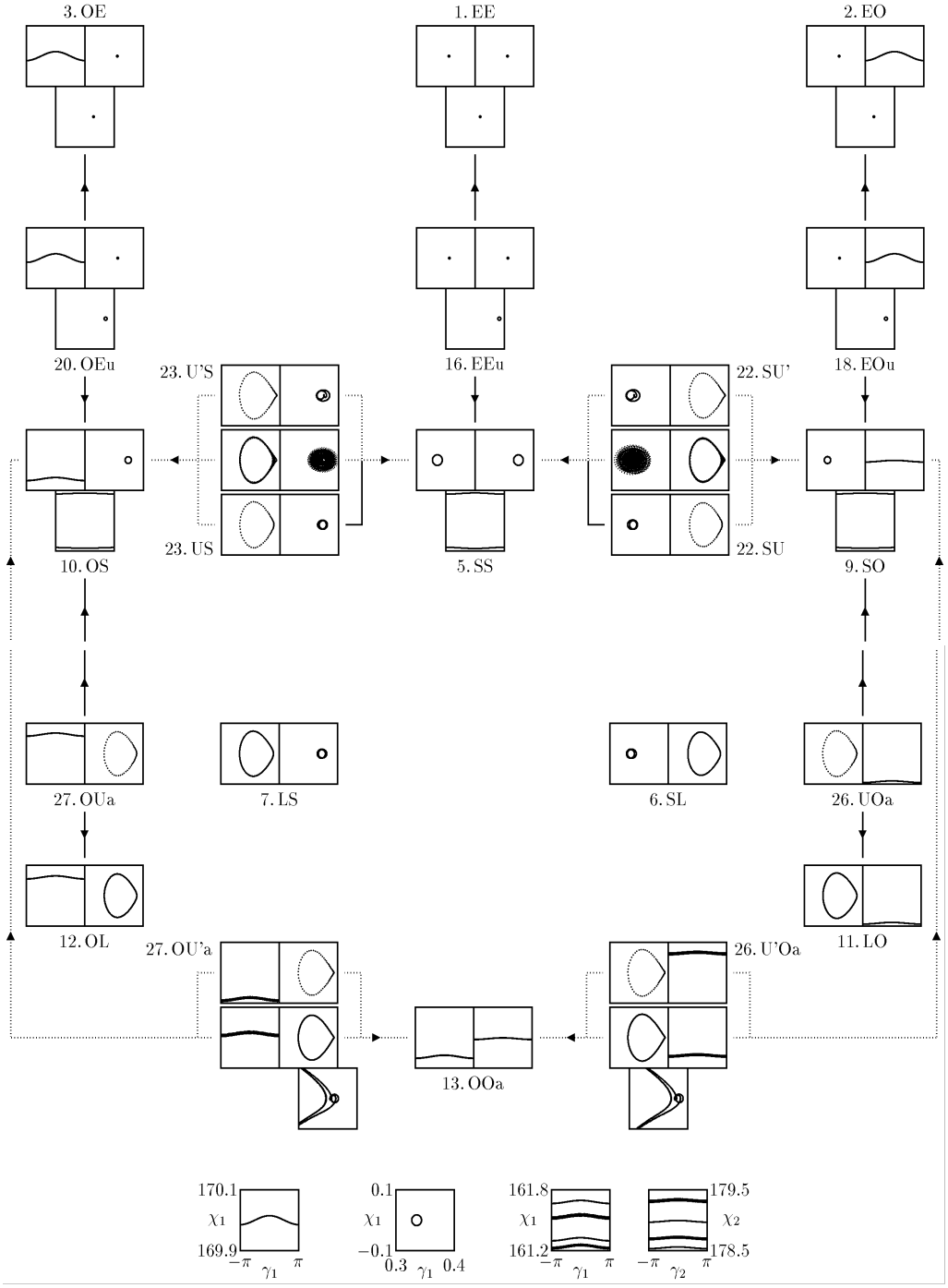

Fig. 9. Connection among steady states for Case 2

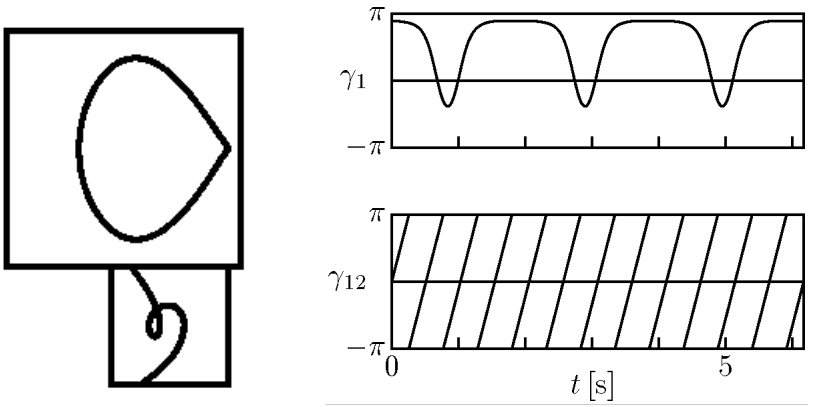

(a) (b)

Fig. 10. A part of the straddle orbit between the OOa and SO

In the case of the straddle orbit between the SS and SL or between the SS and LS, the middle point between a pair of points on the straddle orbit converges to the SO or OS early. When the middle point has converged to the SO or OS, by replacing the middle point with another ratio of dividing, we can get the straddle orbit for a long time relatively. The straddle orbit seems to approach the SU or US before it converges to the SO or OS, it however stays on no closed curves for even one cycle.

5. Conclusion

In this paper we have discussed the connections among steady states of a new mathematical model for an electric power system using straddle orbit methods of computer simulation to find the basic sets. The model, in which there is no infinite bus, nor fixed system frequency, had been introduced in our previous paper. In the simple case of two subsystems (each a swing pair) weakly coupled by an interconnecting transmission line, we had developed a system of seven differential equations which include the variation of frequency in a fundamental way.

Our Case 1 of the model has thirteen attractors and fourteen basic sets, which are unstable steady states with one-dimensional outset. One direction of outset of each basic set is included in basin of some attractor, and the other direction is included in basin of another attractor; connections among steady states are clarified. Also there are seven unstable steady states with two- or three-dimensional outsets, and connections among basic sets and them are clarified. Our Case 2 has eleven attractors and seven basic sets; connections among them are clarified. All unstable steady states with two- or three-dimensional outsets which exist in Case 1 disappear in Case 2.

Our Case 1 is highly idealized, and our Case 2 may correspond more realistically to actual power systems, but many steady states including unstable limit sets observed in Case 1 do not exist in Case 2. Especially, although an unstable equilibrium in a system (a pair of a generator and a motor) is well known as a basic set between normal operation and stepping out, it has disappeared in Case 2. It is another benefit of Case 1 that the role of unstable limit sets which have two- or three-dimensional outsets is clarified. Idealized Case 1 will be important to understand relations among steady states. The limits of applicability of our new model, characterized by the absence of an infinite bus, and its rich field of nonlinear phenomena, awaits further exploration.

6. Acknowledgment

We would like to express our deepest gratitude to Professor Ralph Abraham of the University of California, Santa Cruz, with whom we had been engaged in a series of studies in electric power systems.

References

[1] Ueda Y., Hirano M., Abraham R. H., Ohta H. "Attractor and basin portraits of a double swing power system", [2004] Int. J. of Bifurcation and Chaos 19, 3135-3152.

[2] Battelino P. M., Grebogi C., Ott E., Yorke J. A. "Multiple coexisting attractors, basin boundaries and basic sets", [1988] Phys. D 32, 296-305.